Luminescence properties of Eu^{2+}- and Ce^{3+}-doped $CaAl_2S_4$ and application in white LEDs

Ruijin Yu, Jing Wang*, Jianhui Zhang, Haibin Yuan, Qiang Su*

MOE Laboratory of Bioinorganic and Synthetic Chemistry, State Key Laboratory of Optoelectronic Materials and Technologies, School of Chemistry and Chemical Engineering, Sun Yat-sen University, Guangzhou, Guangdong 510275, PR China

Abstract

The Eu^{2+}- and Ce^{3+}-doped $CaAl_2S_4$ phosphors were comparatively synthesized by conventional solid-state reaction and the evacuated sealed quartz ampoule. The X-ray diffraction (XRD) patterns show that the sample with better crystalline quality was prepared by the evacuated sealed quartz ampoule, resulting in the enhancement of the emission intensity of Eu^{2+} ion by a factor of 1.7. The intensive green LEDs were also fabricated by combining $CaAl_2S_4:Eu^{2+}$ with near-ultraviolet InGaN chips ($\lambda_{em} = 395$ nm). The dependence of as-fabricated green LEDs on forward-bias currents shows that it presents good chromaticity stability and luminance saturation, indicating that $CaAl_2S_4:Eu^{2+}$ is a promising green-emitting phosphor for a near-UV InGaN-based LED. In addition, the optical properties of $CaAl_2S_4:Ce^{3+}$ were systematically investigated by means of diffuse reflectance, photoluminescence excitation and emission, concentrating quenching and the decay curve.
© 2008 Elsevier Inc. All rights reserved.

Keywords: Luminescence; Calcium thioaluminate; Europium; Cerium

1. Introduction

Recently, the ternary compounds $M^{II}M_2^{III}(S,Se)_4$ doped with rare earth ions have attracted much attention for optoelectronic devices such as field emission display (FED), inorganic thin-film electroluminescent (iTFEL) devices, and phosphor converted white light emitting diodes (pc-WLED) [1–7].

In 1992, Le Thi et al. [8] systematically studied the Eu^{2+}-doped MS-Al_2S_3 (M = Ca, Sr, Ba) systems and noted that $BaAl_2S_4:Eu^{2+}$ phosphor had a high efficiency of blue emission. Thereafter, Miura demonstrated the high-luminance blue TFEL device with a new blue-emitting EL phosphor $BaAl_2S_4:Eu^{2+}$ prepared by the two targets pulse-electron-beam evaporation [9]. This blue phosphor with suitable color coordinates, high-enough luminance and efficiency made the full-color device of EL display possible and accelerated iFire Company to announce a full-color

34-in thick dielectric electroluminescent (TDEL) screen using the color-by-blue (CBB) technique [10]. In order to make the CBB approach function effectively, it is essential to develop efficient green and red down-converting phosphors well matching with the efficient thin-film blue-emitting EL device.

$CaAl_2S_4:Eu^{2+}$ is expected to be the promising green candidate for full-color applications [11]. In the past decade, research interest was concerned with the preparation method and fundamental information of $CaAl_2S_4$:Eu^{2+}. Le Thi et al. [8] used alkaline earth sulfides, EuS and Al_2S_3 as starting materials to prepare thioaluminate powders performed in silica tubes sealed under vacuum. Oh et al. [12] prepared $CaAl_2S_4$ single crystals by a chemical transport reaction method in a closed system using high-purity iodine as a transport agent. In addition, thin-film phosphors of $CaAl_2S_4:Eu^{2+},Gd^{3+}$ with a considerably high luminance of 4200 cd/m^2 at 260 V were also electron-beam deposited on substrates using of simultaneous deposition from two source materials, $CaS:Eu^{2+}$, Gd^{3+} and Al_2S_3 [11]. Recently, Van Haecke et al. [13] made use of CaS, Al_2S_3 and EuF_3 as raw materials to

*Corresponding authors. Fax: +86 20 84111038.
E-mail addresses: ceswj@mail.sysu.edu.cn (J. Wang),
Suqiang@mail.sysu.edu.cn (Q. Su).

synthesize the target compound $CaAl_2S_4:Eu^{2+}$ under continuous flow of H_2S and systematically investigate the radiative properties of the phosphor by means of a single-configuration coordinate model.

In this paper, cheap and stable aluminum powder was used as the starting material instead of Al_2S_3 to prepare $CaAl_2S_4:Eu^{2+}$ under a continuous flow of H_2S and under vacuum in sealed silica tubes, respectively. The structure and optical properties of as-synthesized phosphors by two methods were comparatively investigated. The intense green LEDs were first fabricated by combining $CaAl_2S_4$: Eu^{2+} phosphors with 395 nm InGaN UV chips and the dependence of the optical properties of the green LEDs on different forward-bias currents was investigated. Furthermore, the optical properties of Ce^{3+} in calcium thioaluminate were systematically investigated for the first time by means of diffuse reflectance, photoluminescence excitation and emission spectra, concentration quenching and the decay curve.

2. Experimental

2.1. Samples preparation

The starting sulfide materials CaS and EuS were pre-prepared by a solid-state reaction method at high temperature in horizontal tube furnaces. CaS was prepared from $CaCO_3$ (A.R.) under flowing H_2S gas at 1000 °C for 2 h. EuS was prepared from Eu_2O_3 (99.99%) with CS_2 reducing atmosphere at 1200 °C for 2 h. Here, $CaAl_2S_4:RE$ ($RE = Eu^{2+},Ce^{3+}$) phosphor powders were prepared by two different methods:

Method (a): By synthesis from stoichiometric amounts of CaS, Al(A.R.) and EuS or Ce_2S_3, Na_2CO_3(A.R.) and 50 mass% excess S(A.R.) in sealed quartz ampoules at 1050 °C for 5 h. The starting materials (about 0.6 g total mass) were placed in the quartz ampoules (150 mm length, 10 mm inner diameter) and then evacuated to 1×10^{-6} Torr and sealed.

Method (b): By solid-state reaction from mixtures of CaS, Al(A.R.) and EuS or Ce_2S_3, Na_2CO_3(A.R.) in stoichiometric quantities, maintained for 2 h at 1050 °C in a flowing H_2S stream. In the initial and the final heat-treatment stages, the H_2S was replaced by Ar to prevent the possible oxidation of the mixture at temperatures below 700 °C.

2.2. Characterization and optical measurements

The structure of the final products was examined by X-ray powder diffraction using a Rigaku D/max 2200 vpc X-ray Diffractometer with CuKα radiation at 40 kV and 30 mA. The X-ray diffraction (XRD) patterns were collected in the range $10° \leqslant 2\theta \leqslant 70°$ with a scan rate of 4°/min.

The diffuse reflection spectra of the samples were measured by a Cary 5000 UV–Vis–NIR spectrophotometer

equipped with a double out-of-plane littrow monochrom-eter, using $BaSO_4$ as a standard reference in the measure-ments. The photoluminescence (PL), photoluminescence excitation (PLE) spectra of $CaAl_2S_4:RE$ ($RE = Eu^{2+}$, Ce^{3+}) were measured by a Fluorolog-3 spectrofluorometer (Jobin Yvon Inc/specx) equipped with a 450 W Xe lamp and double-excitation monochromators. The decay curves were recorded on an Edinburgh FLS 920 spectrofluorom-eter, equipped with a 450 W xenon lamp, a 150 W nF900 nanosecond flash lamp with a pulse width of 1 ns and a pulse repetition rate of 40–100 kHz. The above measure-ments were carried out at room temperature.

3. Results and discussion

3.1. Phase characterization

Fig. 1 shows the XRD patterns of $CaAl_2S_4:RE$ ($RE = Eu^{2+},Ce^{3+}$) by two different methods. Obviously, a mixture of $CaAl_2S_4$, CaS and Al_2O_3 was formed by method (b). Similar results were also reported in prepara-tion of $CaAl_2S_4$ by using Al_2S_3 as starting materials sintered in a H_2S atmosphere [13]. It is inevitable to introduce the trace amount of air into the sintering system in a flow of freshly prepared H_2S stream. The aluminum powder is very sensitive to oxygen at high temperature. The presence of very stable Al_2O_3 is most probably due to oxidation of a small part of the aluminum powder in the sintering reaction.

The pure $CaAl_2S_4$ phase can be attained by method (a) in evacuated quartz ampoules by heating the stoichiometric amounts of CaS, Al, EuS or Ce_2S_3, Na_2CO_3 with 50 mass% excess S at 1050 °C for 5 h. No other impure phases such as CaS, Al_2S_3 or Al_2O_3 were detected, which is in good agreement with the JCPDS card (No. 77–1186). The lattice constants of phosphors are calculated to be $a = 20.003$ Å, $b = 20.588$ Å, $c = 11.909$ Å, $V = 4904.56$ Å^3
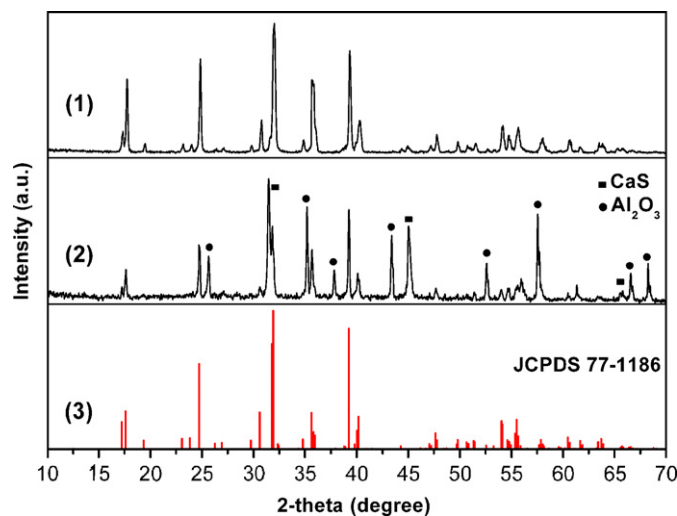

Fig. 1. XRD patterns of the $CaAl_2S_4:Eu^{2+}$: (1) prepared by method (a); (2) prepared by method (b); (3) JCPDS card (No. 77–1186).

for CaAl$_2$S$_4$:Eu^{2+}; $a = 19.892$ Å, $b = 20.644$ Å, $c = 11.892$ Å, $V = 4883.46$ Å^3 for CaAl$_2$S$_4$:Ce^{3+}, Na$^+$, which are consistent with the reported lattice constants $a = 20.163$ Å, $b = 20.052$ Å, $c = 12.026$ Å, $V = 4862.21$ Å^3 of CaAl$_2$S$_4$ [14]. Considering the ionic radii of Ca^{2+}(112 pm), Eu^{2+}(125 pm) and Ce^{3+}(114 pm) ions in site of CN = 8, it is reasonable that the unit cell of CaAl$_2$S$_4$ expands when Ca^{2+} ions are substituted by Eu^{2+} ions or Ce^{3+} ions. This result implies that the dopant ions are incorporated into the structure of CaAl$_2$S$_4$. In summary, aluminum powder can be used as a cheap and stable starting material for preparation of CaAl$_2$S$_4$ instead of expensive and weakly hygroscopic Al$_2$S$_3$ and the method (a) by evacuated quartz ampoules used in the present case is necessary to access excellent crystalline CaAl$_2$S$_4$ powders.

3.2. The luminescence properties of CaAl$_2$S$_4$:RE (RE = Eu^{2+}, Ce^{3+})

Fig. 2 presents the diffuse reflectance and the absorption spectra of CaAl$_2$S$_4$, CaAl$_2$S$_4$:Eu^{2+} and CaAl$_2$S$_4$:Ce^{3+}, Na$^+$ phosphors. The absorption spectra $F(R)$ were obtained from the diffuse reflection spectra by using the Kubelka–Munk function [15]:

$$F(R) = (1 - R)^2/2R = K/S, \qquad (1)$$

where R, K and S are the reflectivity, the absorption coefficient and the scattering coefficient, respectively. It is clear that the CaAl$_2$S$_4$ host shows a platform of nearly 65–70% diffuse reflectance in the wavelength range of 500–650 nm (curve 1). When europium and cerium ions are doped into the host, several obvious broad bands are induced in the wavelength range of 260–520 nm, due to the $4f \rightarrow 5d$ transition of Eu^{2+} and Ce^{3+} ions. The absorption coefficient of CaAl$_2$S$_4$:Eu^{2+} around 300 nm (curve 3 in Fig. 2) is larger than that of the host material. This implies that the absorption of Eu^{2+}-doped CaAl$_2$S$_4$ around
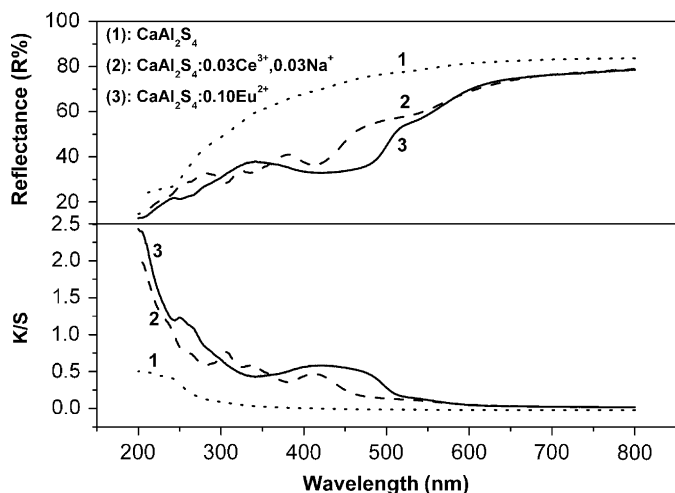
300 nm partially originated from the $4f \rightarrow 5d$ transition of Eu^{2+}. The host absorption edge is determined to be around 300 nm (4.13 eV), essentially due to the valence to conduction band transitions of the host.

The excitation and emission spectra of CaAl$_2$S$_4$:10 mol%Eu^{2+} phosphor prepared by two different methods are shown in Fig. 3. For the sample prepared by method (a), the excitation spectrum of curves exhibits several broad bands around 280, 332, 384 and 454 nm, which are attributed to the host absorption and the $4f^7(^8S_{7/2}) \rightarrow 4f^6(^7F)5d^1$ transitions of Eu^{2+} ion, and consistent with the diffuse reflectance spectra as presented in Fig. 2. For the emission spectrum, a predominating band with the full-width at half-maximum (FWHM) about 37 nm is around 516 nm, ascribed to the $4f^6(^7F)5d^1 \rightarrow 4f^7(^8S_{7/2})$ allowed transition of Eu^{2+} ions. For the sample prepared by method (b), there are some impurities such as CaS and Al$_2$O$_3$ in the sintered powder. However, a small amount of CaS:Eu^{2+} in the sintered powder has a negligible emission at 650 nm, as it has a low efficiency at Eu^{2+} concentrations higher than 0.2 mol%. Al$_2$O$_3$:Eu^{3+} powder is characterized by Eu^{3+} emission lines [13]. Both the spectra characteristics of CaS:Eu^{2+} and Al$_2$O$_3$:Eu^{3+} were not observed in curve (2) of Fig. 3. So the presence of impurities in the powder has no influence on the spectrum shape of the CaAl$_2$S$_4$:Eu^{2+} phosphor.

It can be comparatively observed in Fig. 3 that the phosphor prepared by method (a) presents more intense excitation bands in the wavelength range from 250 to 500 nm, especially the host absorption band around 280 nm. And the emission intensity of Eu^{2+} ion in the sample synthesized by method (a) is by a factor of 1.7 as strong as that of Eu^{2+} ion in the sample prepared by method (b). The distinct optical features are ascribed to the improved crystalline quality as mentioned in the phase characterization.
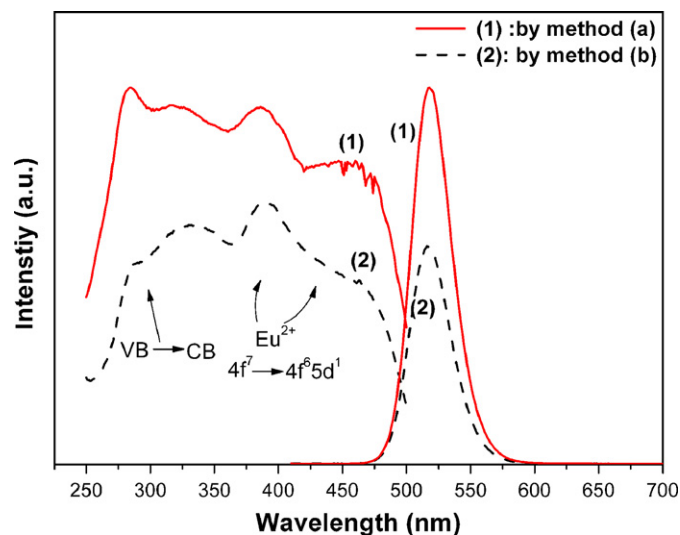

Fig. 2. The diffuse reflectance and the absorption spectra of CaAl$_2$S$_4$, CaAl$_2$S$_4$:0.10Eu^{2+} and CaAl$_2$S$_4$:0.03Ce^{3+}, 0.03Na$^+$ phosphors prepared by the method (a).

Fig. 3. PL emission ($\lambda_{ex} = 395$ nm) and excitation ($\lambda_{em} = 516$ nm) spectra of CaAl$_2$S$_4$:Eu^{2+} (10 mol%) prepared by the method (a) for curve (1) and method (b) for curve (2).

The emission and excitation spectra of Ce^{3+} in $CaAl_2S_4$ are presented in Fig. 4 at room temperature. It is obvious that Ce^{3+} ion shows two well-resolved emission bands at 436 nm (22936 cm^{-1}) and 477 nm (20964 cm^{-1}), corresponding to the transition of 5d-excited state to $^2F_{5/2}$ and $^2F_{7/2}$ of Ce^{3+} ion. The energy difference is about 1972 cm^{-1}. The excitation spectra of Ce^{3+} in $CaAl_2S_4$ consist of three broad bands at around 277, 320 and 404 nm in the range of 240–420 nm, monitoring at 436 nm emission. They are attributed to the $4f \rightarrow 5d$ transition of Ce^{3+} and consistent with the diffuse reflectance spectra. The value of the red shift (D) expressed by the energy difference of the lowest 5d-excited levels of Ce^{3+} in the present host compared with the free ion of Ce^{3+} is 24588 cm^{-1}. The Stokes shift is calculated to be 1636 cm^{-1}. It is weaker in $CaAl_2S_4:Ce^{3+}$ compared to the value found in $CaGa_2S_4:Ce^{3+}$ ($S = 0.24\,eV = 1935\,cm^{-1}$) [16].

Furthermore, Dorenbos [17] also proposed a relationship correlating the $4f$–$5d$ energies of Ce^{3+} and Eu^{2+} ions in the same lattice site of a specific host:

$$E(Eu^{2+}) = (0.64 \pm 0.02) \times E(Ce^{3+}) + (0.53 \pm 0.06)\,eV, \tag{2}$$

where $E(Eu^{2+})$ and $E(Ce^{3+})$ are the energies of the lowest f–d transition absorption of Eu^{2+} and Ce^{3+}, respectively. Using this equation, the lowest 5d crystal-field splitting component of Eu^{2+} in $CaAl_2S_4$ is estimated to be $2.50 \pm 0.12\,eV$, i.e. in the range of 473–521 nm, showing an agreement with the results obtained by using the mirror–image relationship between the emission and the excitation spectrum [13].

It is reported that the emission peaks are located at 553 nm and 468, 517 nm for Eu^{2+}- and Ce^{3+}-doped $CaGa_2S_4$, respectively [16,18]. In the present case, Eu^{2+}-
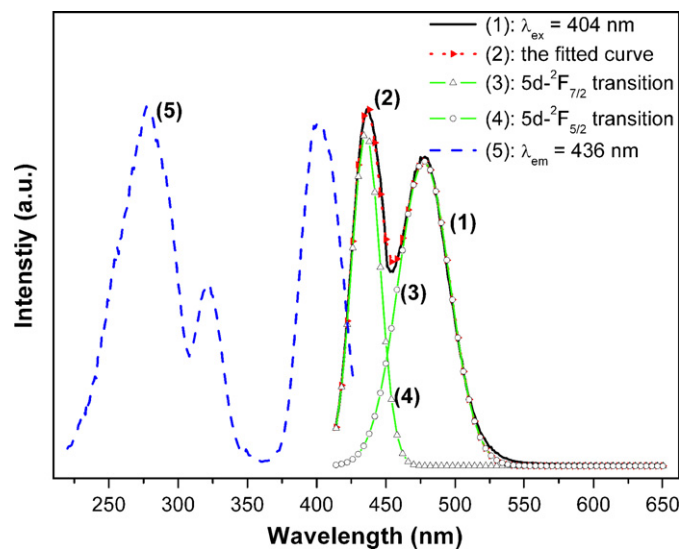
and Ce^{3+}-doped $CaAl_2S_4$ compounds exhibit obvious blue shift compared to $CaGa_2S_4$ compounds. Such a blue shift is mainly ascribed to the difference in the distance of the Ca–S bond in these compounds. The compounds $CaAl_2S_4$ and $CaGa_2S_4$ are isomorphic, both of which show an orthorhombic crystal structure. The average distance of the Ca–S bond in $CaAl_2S_4$ is 3.023 Å, longer than that (3.015 Å) in $CaGa_2S_4$ [14]. Therefore, Eu^{2+} or Ce^{3+} ions in $CaAl_2S_4$ have weaker crystal fields rather than in $CaGa_2S_4$, indicating that the lowest 5d-excited level of Eu^{2+} or Ce^{3+} ions is higher in $CaAl_2S_4$ than that in $CaGa_2S_4$. The same blue shift behavior is also observed in Eu^{2+}-doped $M^{II}M_2^{III}S_4$. The crystal field splitting of Eu^{2+} 5d orbitals by the S^{2-} anions in these $M^{II}M_2^{III}S_4$ compounds decreases with the decreasing size of M^{III} (In, Ga, Al) and with the increasing size of the M^{II} cation (Ca, Sr, Ba) [19,20].

The influence of the europium and cerium concentration on the luminescence process was investigated as shown in Fig. 5. The PL intensity increases with the doped ions content increasing until it reaches a maximum intensity at about 3 and 10 mol% for Ce^{3+} and Eu^{2+}, respectively. And then it decreases because of concentration quenching. The observed optimum europium concentration for $Ca_{1-x}Eu_xAl_2S_4$ is generally identical with previous data [8,13].

The fluorescence decay times of Eu^{2+} and Ce^{3+} emissions at room temperature are shown in Fig. 6, the decay curves can be well fitted by a single exponential equation:

$$I_t = I_0 \exp(-t/t), \tag{3}$$

where I_t and I_0 are the luminescence intensities at time t and 0, respectively, and τ is the decay time. The values of τ are calculated to be 0.48 μs and 24.2 ns from the fitted curves for the samples $Ca_{0.90}Eu_{0.10}Al_2S_4$ and $Ca_{0.94}Ce_{0.03}$

Fig. 4. PL emission [(1), $\lambda_{ex} = 404$ nm] and excitation [(5), $\lambda_{em} = 436$ nm] spectra of $CaAl_2S_4:Ce^{3+}$ (3 mol%), Na^+ (3 mol%) prepared by the method (a) [(2), the fitted curve of curve (1); (3) and (4), the deconvoluted curves of curve (1)].
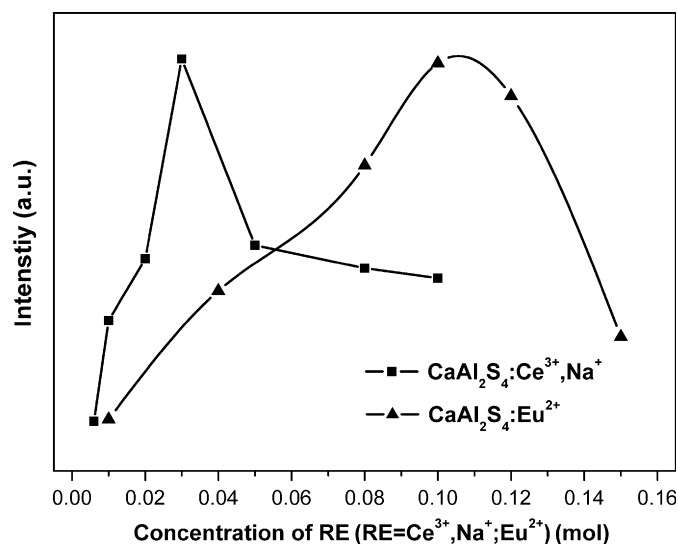
Fig. 5. Dependence of PL intensities of $Ca_{1-x}Eu_xAl_2S_4$ ($\lambda_{ex} = 395$ nm, $\lambda_{em} = 516$ nm) on Eu^{2+} content and $Ca_{1-2x}Ce_xNa_xAl_2S_4$ ($\lambda_{ex} = 404$ nm, $\lambda_{em} = 436$ nm) on Ce^{3+} content prepared by the method (a).
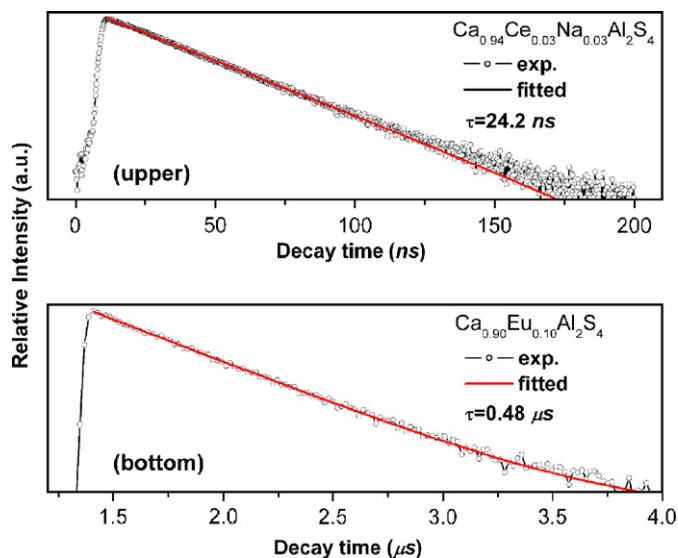
Fig. 6. The decay curves of $Ca_{0.90}Eu_{0.10}Al_2S_4$ (bottom: $\lambda_{ex} = 395\,nm$, $\lambda_{em} = 516\,nm$) and $Ca_{0.94}Ce_{0.03}Na_{0.03}Al_2S_4$ (upper: $\lambda_{ex} = 404\,nm$, $\lambda_{em} = 436\,nm$) prepared by the method (a).

$Na_{0.03}Al_2S_4$, respectively. The lifetime value of Eu^{2+} in $CaAl_2S_4{:}0.10Eu^{2+}$ is comparable to the reported value $0.40\,\mu s$ in Ref. [13]. The lifetime value of Ce^{3+} in $Ca_{1-2x}Ce_xNa_xAl_2S_4$ is in the range of nanosecond, which is also reasonable for the $5d$–$4f$-allowed transition of Ce^{3+} [21].

3.3. Fabricated LEDs with $CaAl_2S_4{:}Eu^{2+}$ phosphor

As shown in Figs. 3 and 4, the broad excitation bands of $CaAl_2S_4{:}RE$ ($RE = Eu^{2+}, Ce^{3+}$) phosphors match well with n-UV light emitted by the InGaN LED, indicating a potential application of these phosphors in an n-UV LED chip. It is necessary to investigate the optical properties of these phosphor in a device combined with an n-UV Ga(In)N chip. Compared with the $CaAl_2S_4{:}Ce^{3+}$ phosphor, the $CaAl_2S_4{:}Eu^{2+}$ phosphor shows much more emission intensity in our experiments. For this purpose, a 395-nm Ga(In)N chip is used to fabricate the single-color LED based on $CaAl_2S_4{:}Eu^{2+}$ phosphor. Fig. 7 is the electroluminescence spectra of the naked n-UV LED and as-fabricated PC-LED at $I_F = 20\,mA$. Two distinct emission bands around 395 and 516 nm are clearly observed in the emission spectrum of the PC-LED. From two curves, it is obviously observed that the near-violet light of the naked n-UV-LED chip at 395 nm is absorbed dramatically by the $CaAl_2S_4{:}Eu^{2+}$ (curve 2) and simultaneously down-converted into an intensive green light around 516 nm. Its color coordinates are about (0.158, 0.658) at $I_F = 20\,mA$.

Fig. 8 shows the dependence of the color coordinates of the as-fabricated green LED on different forward-bias currents ($I_F = 5.0, 10, 20, 30, 40$ and $50\,mA$) plotted in the CIE 1931 chromaticity diagram. As the drive current increases, there are a few changes in color coordinates and in the FWHM of the emission. The color coordinates of the
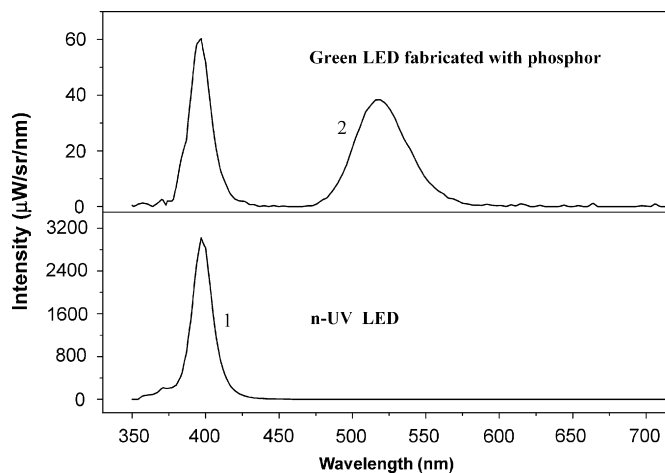

Fig. 7. The electroluminescence spectra of a naked UV LED (curve 1) and the fabricated PC-LED (curve 2) combined with $CaAl_2S_4{:}Eu^{2+}$ phosphor prepared by the method (a) under 20-mA forward-bias current.

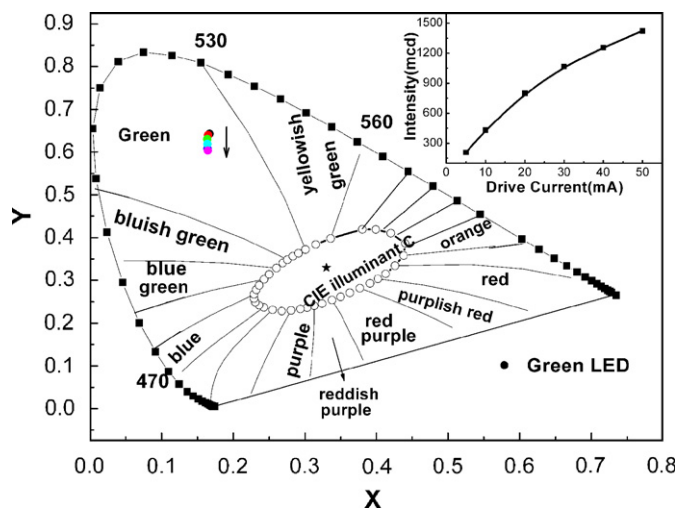Fig. 8. The CIE coordinates of PC-LEDs based on $CaAl_2S_4{:}Eu^{2+}$ prepared by the method (a) under $I_F = 5.0, 10, 20, 30, 40$ and $50\,mA$ in the CIE 1931 chromaticity diagram. The inset shows the dependence of the emission intensity on forward-bias currents.

fabricated LED shift slightly as shown in Fig. 8 with the circle symbols. The X value of color coordinates decreases slightly, approximately difference percentage of -1.3%, and the Y value of color coordinates decreases a little, approximately difference percentage of -6%. The FWHM of the emission bands are 42, 42, 42, 43, 43 and 44 nm, respectively. As is shown in the inset, the relative intensity of the fabricated LED increases with the forward-bias current increasing from 5 to 50 mA, it tends to no significant saturation or quenching phenomenon, even the operation current is over 50 mA. The dependence of as-fabricated green LED on forward-bias currents shows that it presents good chromaticity stability and luminance saturation, indicating that $CaAl_2S_4{:}Eu^{2+}$ is a promising green-emitting phosphor for a near-UV InGaN-based white LED.

4. Conclusions

In this work, the phosphors $CaAl_2S_4$:RE ($RE = Eu^{2+}$, Ce^{3+}) have been comparatively synthesized by conventional solid-state reaction and the evacuated sealed quartz ampoule. The samples synthesized by the evacuated sealed quartz ampoule show better crystalline quality and stronger emission intensity. The optimal concentration for Ce^{3+} and Eu^{2+} in $CaAl_2S_4$ is about 3 and 10 mol%, respectively. The intensive green LEDs were fabricated by combining the synthesized phosphor ($CaAl_2S_4$:Eu^{2+}) with near-ultraviolet InGaN chips ($\lambda_{em} = 395$ nm). It is believed to be a good green phosphor candidate for white LED application.

Acknowledgments

Reference

[1] T.E. Peters, J.A. Baglio, J. Electrochem. Soc. 119 (1972) 230–236.
[2] L. Eichenauer, B. Jarofke, H.C. Mertins, et al., Phys. Status Solidi A 153 (2) (1996) 515–527.
[3] Ronot-Limousin, A. Garcia, C. Fouassier, et al., J. Electrochem. Soc. 144 (1997) 687–694.
[4] S. Yang, C. Stoffers, F. Zhang, B.K. Wagner, et al., Appl. Phys. Lett. 72 (1998) 158–160.
[5] P. Benalloul, C. Barthou, J. Benoit, J. Alloy. Compd. 275–277 (1998) 709–714.
[6] R. Mueller-Mach, G.O. Mueller, Proc. SPIE 3938 (2000) 30–41.
[7] Y.R. Do, K.Y. Ko, S.H. Na, et al., J. Electrochem. Soc. 153 (2006) H142–H146.
[8] K.T. Le Thi, A. Garcia, F. Guillen, et al., Mater. Sci. Eng. B—Solid 14 (1992) 393–397.
[9] N. Miura, M. Kawanishi, H. Matsumoto, et al., Jpn. J. Appl. Phys. Part 2 38 (1999) L1291–L1292.
[10] X. Wu, A. Nakua, D. Cheong, J. Soc. Inf. Display 12 (3) (2004) 281–286.
[11] A. Nakua, D. Cheong, X. Wu, J. Soc. Inf. Display 11 (3) (2003) 493–498.
[12] S.K. Oh, H.J. Song, W.T. Kim, et al., J. Phys. Chem. Solids 61 (2000) 1243–1247.
[13] J.E. Van Haecke, P.F. Smet, D. Poelman, J. Lumin. 126 (2007) 508–514.
[14] B. Eisenmann, M. Jakowski, W. Klee, et al., Rev. Chim. Miner. 20 (1983) 255–263.
[15] G. Kortum, G. Schreyer, Z. Naturforsch. A: Phys. Sci. 11 (1957) 1018–1022.
[16] A. Kato, M. Yamazaki, H. Najafov, et al., J. Phys. Chem. Solids 64 (2003) 1511–1517.
[17] P. Dorenbos, J. Phys.: Condens. Matter. 15 (2003) 4797–4807.
[18] P. Benalloul, C. Barthou, C. Fouassier, et al., J. Electrochem. Soc. 150 (1) (2003) 62–65.
[19] P.C. Donohue, J.E. Hanlon, J. Electrochem. Soc. 121 (1974) 137–142.
[20] R.B. Jabbarov, C. Chartier, B.G. Tagiev, et al., J. Phys. Chem. Solid 66 (2005) 1049–1056.
[21] G. Blasse, B.C. Grabmaier, Luminescent Materials, Springer, Berlin, Heidelberg, 1994.